Decay of a microsecond seniority 3 isomeric state in ^{155}Hf

B. Alayed,[1,2] R. D. Page,[2] D. T. Joss,[2] J. Uusitalo,[3,2] C. Qi,[4] A. D. Briscoe,[2,3] M. A. M. AlAqeel,[5,2] B. Andel,[6] S. Antalic,[6] K. Auranen,[3] H. Ayatollahzadeh,[7] H. Badran,[3] L. Barber,[8] G. Beeton,[7] M. Birova,[9] V. Bogdanoff,[3] J. G. Cubiss,[10] D. M. Cullen,[8] J. Deary,[7] U. Forsberg,[3] T. Grahn,[3] P. T. Greenlees,[3] J. B. Hilton,[2,3] A. Illana,[3] H. Joukainen,[3] D. S. Judson,[2] R. Julin,[3] H. Jutila,[3] J. M. Keatings,[7] M. Labiche,[11] M. Leino,[3] M. C. Lewis,[2] J. Louko,[3] M. Luoma,[3] I. Martel,[2,12] A. McCarter,[2] P. P. McKee,[7] P. Mosat,[6] S. N. Nathaniel,[2] O. Neuvonen,[3] D. O'Donnell,[7] J. Ojala,[3] C. A. A. Page,[10] A. M. Plaza,[2,3] J. Pakarinen,[3] P. Papadakis,[11] E. Parr,[2] J. Partanen,[3] P. Rahkila,[3] J. Romero,[2,3] P. Ruotsalainen,[3] M. Sandzelius,[3] J. Sarén,[3] B. Saygi,[13,14] J. Smallcombe,[2,15] J. F. Smith,[7] J. Sorri,[16] C. M. Sullivan,[2] S. Szwec,[3] H. Tann,[2,3] A. Tolosa-Delgado,[3] E. Uusikylä,[3] M. Venhart,[9] L. J. Waring,[2] and G. Zimba[3,17]

[1]*Department of Physics, College of Science, Qassim University, Buraydah 51452, Saudi Arabia*
[2]*Department of Physics, Oliver Lodge Laboratory, University of Liverpool, Liverpool L69 7ZE, United Kingdom*
[3]*Accelerator Laboratory, Department of Physics, University of Jyväskylä, FI-40014 Jyväskylä, Finland*
[4]*Department of Physics, Royal Institute of Technology, Alba Nova Centre, S-106 91 Stockholm, Sweden*
[5]*Physics Department, Imam Mohammad Ibn Saud Islamic University, 90950, Riyadh 11623, Saudi Arabia*
[6]*Department of Nuclear Physics and Biophysics, Comenius University in Bratislava, 84248 Bratislava, Slovakia*
[7]*School of Computing, Engineering, and Physics Sciences, University of the West of Scotland, Paisley PA1 2BE, United Kingdom*
[8]*Department of Physics and Astronomy, Schuster Building, The University of Manchester, Manchester M13 9PL, United Kingdom*
[9]*Institute of Physics, Slovak Academy of Sciences, 84511 Bratislava, Slovakia*
[10]*School of Physics, Engineering and Technology, The University of York, York YO10 5DD, United Kingdom*
[11]*Daresbury Laboratory, Science and Technology Facilities Council, Warrington WA4 4AD, United Kingdom*
[12]*Faculty of Experimental Sciences, University of Huelva, 21071 Huelva, Spain*
[13]*Institute of Nuclear Sciences, Ankara University, Ankara, Türkiye*
[14]*Nuclear Energy Research Institute, Turkish Energy Nuclear and Mineral Research Agency, Ankara, Türkiye*
[15]*Advanced Science Research Center, Japan Atomic Energy Agency (JAEA), Tokai, Ibaraki 319-1195, Japan*
[16]*Sodankylä Geophysical Observatory, University of Oulu, FIN-99600 Sodankylä, Finland*
[17]*Facility for Rare Isotope Beams, Michigan State University, East Lansing, Michigan 48824, USA*

(Received 2 May 2024; revised 29 July 2024; accepted 13 August 2024; published 3 September 2024)

Excited states in the neutron-deficient nuclide ^{155}Hf have been investigated in experiments performed at the Accelerator Laboratory of the University of Jyväskylä. The ^{155}Hf nuclei were produced in fusion-evaporation reactions induced by beams of 295 and 315 MeV ^{58}Ni ions bombarding an isotopically enriched ^{102}Pd target and separated using the recoil mass separator MARA. An isomeric state having a half-life of 510(30) ns was discovered and is interpreted as a seniority $\upsilon = 3$, $(\pi h_{11/2}^2 \otimes \nu f_{7/2})27/2^-$ configuration. The γ-ray transitions emitted in the deexcitation of the isomeric state to the ground state were identified and a level scheme was constructed, from which the excitation energy of the isomer was determined to be 2581.5(10) keV. A $B(E2)$ value of 0.45(3) W.u. was deduced for the 105.4 keV transition depopulating the isomeric state. The deduced level scheme and $B(E2)$ value are compared with systematics and shell-model calculations.

DOI: 10.1103/PhysRevC.110.034303

I. INTRODUCTION

Isomeric states have long been a valuable source of information on atomic nuclei across the Segrè chart [1]. In nuclei near closed shells, seniority isomers [2] can be formed by the successive alignment of particles in high-j orbitals. The longevity of maximally aligned configurations arises from the roughly inverted parabolic variation of level energies with increasing spin, which can be augmented by the reduction in $E2$ transition strengths because of seniority cancellation as the relevant orbital becomes half-filled. These energetically favored states often have relatively pure configurations, thereby providing an important testing ground for shell-model calculations.

Examples of such seniority isomers have been found near the $N = 82$ shell closure, with configurations having protons in the $\pi h_{11/2}$ orbital. The seniority $\upsilon = 2$, yrast $(\pi h_{11/2}^2)10^+$ states in the even-A $N = 82$ isotones ^{148}Dy [3–5], ^{150}Er [6,7], ^{152}Yb [7,8], and ^{154}Hf [9,10] all decay by $E2$ transitions, as do the $\upsilon = 3$, yrast $(\pi h_{11/2}^3)27/2^-$ states in the odd-A isotones ^{149}Ho [11,12], ^{151}Tm [6,8], and ^{153}Lu [9,10]. The

measured half-lives range from 59 ns for ^{149}Ho to 34 μs for ^{152}Yb, while the transition energies, where known, decrease with increasing Z for both seniorities. The resulting $E2$ transition strengths deduced from the measurements are consistent with simple shell-model predictions [13] and suggest that the $\pi h_{11/2}$ orbital is half-filled at $Z = 71$ (Lu) [9,10].

In the odd-A $N = 81$ isotones ^{147}Dy [14], ^{149}Er [15], and ^{151}Yb [7,16] the yrast $\upsilon = 3$ $(\pi h^2_{11/2} \otimes \nu h^{-1}_{11/2})27/2^-$ states are isomeric, also decaying by $E2$ transitions. However, the 10^+ isomers in the odd-odd $N = 81$ isotones ^{146}Tb, ^{148}Ho, and ^{150}Tm [12,17,18] behave differently, decaying by $E3$ transitions with millisecond half-lives. They are interpreted as having a $\upsilon = 2$ $(\pi h_{11/2} \otimes \nu h^{-1}_{11/2})$ structure.

Isomers have also been observed in the $N = 83$ isotones, with an unpaired $f_{7/2}$ neutron coupled to the proton configuration. Although the $\upsilon = 3$ $(\pi h^2_{11/2} \otimes \nu f_{7/2})27/2^-$ isomer in ^{153}Yb decays with a 15 μs half-life via an $E2$ transition like the $N = 82$ isotones [10,19], the corresponding isomers in ^{149}Dy [4,20,21] and ^{151}Er [21–23] have half-lives of ≈0.5 s and decay instead mainly by internal $E3$ transitions with small competing β-decay branches. The $\upsilon = 4$ $(\pi h^3_{11/2} \otimes \nu f_{7/2})17^+$ isomers in the odd-odd isotones ^{150}Ho [24], ^{152}Tm [24], and ^{154}Lu [9,10,25] behave similarly to the $27/2^-$ isomers in their respective $N = 82$ isotopes, decaying via $E2$ transitions.

Of the isomers discussed above, those in ^{153,154}Lu have the smallest known $E2$ transition strengths, with $B(E2)$ values of 0.45(9) and 0.19(2) e^2fm^4, respectively [9,10,25]. However, the depopulating transition energies for ^{153}Yb and ^{154}Hf could not be measured, so the $B(E2)$ values are only estimates for these cases straddling the point where the $\pi h_{11/2}$ orbital is thought to be half-filled and seniority cancelling occurs [2]. For these seniority isomers close to $N = 82$, no $B(E2)$ values have been measured in any nuclide with $Z > 71$, where they are expected to increase again and a measurement could unambiguously establish the minimum.

The next $N = 83$ isotone above ^{154}Lu is ^{155}Hf, but prior to the present work only the half-life of its β-decaying ground state was known [26,27]. In this work, a microsecond isomer has been identified and assigned as the $\upsilon = 3$ $(\pi h^2_{11/2} \otimes \nu f_{7/2})27/2^-$ isomer in ^{155}Hf. A level scheme has been constructed on the basis of the measured γ-ray intensities, γ-γ coincidences, and comparisons with neighboring nuclei. The energy of the $E2$ transition depopulating the isomer has been identified and combining this information with the measured half-life has allowed the $B(E2)$ value to be deduced for a seniority isomer with a more than half-filled $\pi h_{11/2}$ orbital. The level scheme and the $B(E2)$ value are compared with shell-model calculations performed using an interaction optimised for this region of the nuclear chart that was used previously for excited states in the adjacent isobar ^{155}Lu [28].

II. EXPERIMENTAL DETAILS

The ^{155}Hf nuclei were produced in the fusion-evaporation reaction ^{102}Pd(^{58}Ni, $2p3n$)^{155}Hf in two separate measurements at the Accelerator Laboratory of the University of Jyväskylä. The ^{58}Ni beam provided by the K130 cyclotron bombarded the self-supporting isotopically enriched ^{102}Pd target foil of thickness 1 mg/cm^2. Beam energies at the front of the target of 295 and 315 MeV were used for periods of 118 and 155 hours, respectively, with intensities of 3–5 particle nA. The cross section for the production of ^{155}Hf is expected to be similar to that for ^{159}W produced in the reaction ^{106}Cd(^{58}Ni, $2p3n$), which was estimated in a previous study to be ≈10 μb [27].

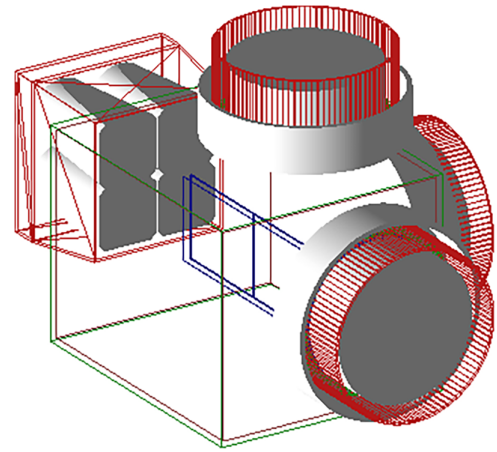

FIG. 1. GEANT4 visualization of the arrangement of the Ge detectors at the focal plane of MARA. The evaporation residues emerged from the MARA separator from the left and were implanted into the DSSD shown in the blue outline. The clover detector was mounted to the left of the DSSD as viewed from the beam direction, and the BEGe detectors were mounted above, behind, and to the right of the DSSD. The vacuum chamber is indicated by the cuboid outline.

The ^{155}Hf ions recoiled out of the target, passed through a carbon foil of nominal thickness 50 μg/cm^2 mounted ≈10 cm downstream of the target to reset the ionic charge-state distribution of the evaporation residues, and were transported using the Mass Analysing Recoil Apparatus (MARA) [29–32]. The flight time to the focal plane of MARA was estimated to be ≈0.6 μs. The ions passed through a multiwire proportional counter (MWPC) and were implanted into a double-sided silicon strip detector (DSSD). The energy signal in the DSSD and the time of flight between the MWPC and the DSSD allowed evaporation residues to be distinguished from beamlike particles. The DSSD had an active area of 128 mm × 48 mm and was 300 μm thick. The strips on its front and back surfaces were orthogonal and the strip pitch of 0.67 mm on both faces provided 13824 pixels.

A clover detector and three broad-energy germanium (BEGe) detectors were mounted around the vacuum chamber enclosing the MWPC and DSSD to measure the energies of x rays and γ rays. The arrangement of the Ge detectors at the focal plane is illustrated in Fig. 1. The distances of the front surfaces of the Ge detectors to the center of DSSD were 7 cm for the top BEGe detector, 6 cm for the BEGe detector mounted behind the DSSD, and 10.5 cm for both the clover detector and the BEGe detector mounted to the right of the DSSD. The prompt time response peaks for the Ge detectors at 122 keV were found to be well approximated by a Gaussian distribution using a ^{152}Eu calibration source. The

clover detector and BEGe detector peaks had full widths at half maximum of ≈70 ns and ≈400 ns, respectively.

Determining the intensities of γ-ray transitions of nuclei implanted into the DSSD requires knowledge of the detector efficiencies for their extended spatial distributions. To achieve this, the absolute efficiencies of the detectors were first measured using a standard ^{152}Eu and ^{133}Ba calibration source. These efficiencies were modeled using GEANT4 [33] to ensure the correct materials were included in the simulations. The simulations were then extended to model γ-ray emissions from the isomeric states in ^{153}Yb, ^{156}Lu, and ^{158}Ta produced in the experiment, using the spatial distributions measured in the DSSD. The γ-ray intensities deduced using the simulated efficiencies were found to be consistent with the literature values [10,34–36]. The efficiency of the Ge detector array for the extended source distributions in the DSSD was found to have a maximum of ≈27 % at 90 keV, reducing to ≈5% at 1 MeV. The efficiencies of the individual Ge detectors were sufficiently low that summing losses were not significant compared with the statistical uncertainties.

Charged particles emitted at the target position during evaporation-residue formation were detected using JYTube [37], which comprised 120 plastic scintillator detectors arranged in a hexagonal-cylindrical geometry. Each detector was 2 mm thick and was directly coupled to a silicon photomultiplier on its back surface. The efficiency of JYTube for detecting a single proton was estimated to be ≈70%. Analyzing the yields of γ rays as a function of the number of hits recorded in JYTube allowed assignments of the atomic number to be made for different isomeric states. Also surrounding the target position were 14 Compton-suppressed Ge detectors that were used to measure prompt γ radiation emitted by the recoiling evaporation residues. These single-crystal Ge detectors were a subset of the JUROGAM3 spectrometer and were deployed in rings at angles of 133.6° and 157.6° to the beam direction [38].

All detector signals were passed to the triggerless data acquisition system [39], where they were time stamped with a precision of 10 ns. The data were analysed using the GRAIN [40] software package.

III. RESULTS

Selecting the ^{155}Hf nuclei produced in the experiment is challenging because it is produced with a much lower cross section than its less exotic isobars and, unlike α emitters, there is no characteristic energy signal provided by its β decays. However, the β decay of ^{155}Hf is known to populate both the $\pi h_{11/2}$ ground state [$E_\alpha = 5655(5)$ keV, $t_{1/2} = 70(1)$ ms] and low-lying $\pi s_{1/2}$ isomeric state [$E_\alpha = 5584(5)$ keV, $t_{1/2} = 136(9)$ ms] of ^{155}Lu [27,41]. The half-life of ^{155}Hf was determined indirectly to be 840(30) ms by analyzing the time differences between the observation of α decays of ^{159}W and ^{155}Lu [26,27]. Therefore correlations with ^{155}Lu α decays that were delayed by the intervening β decays can be used to assign isomeric γ decays to ^{155}Hf. The energy spectrum of α particles used for selecting the ^{155}Hf isomeric decays is shown in Fig. 2(a).

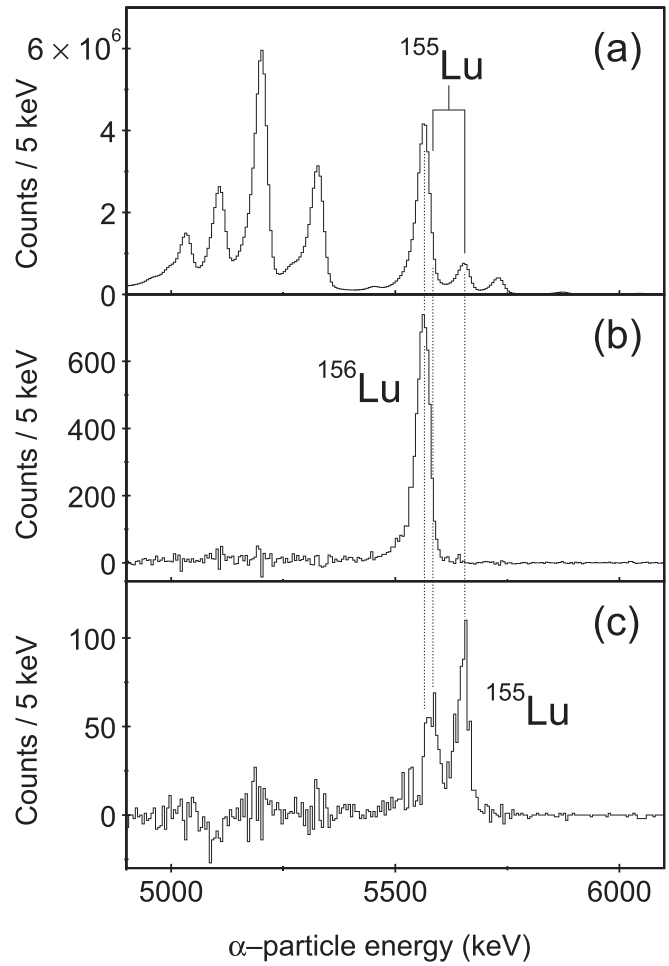

FIG. 2. (a) Energy spectrum of α particles occurring within 4.5 s of the implantation of an ion into the same DSSD pixel. The energies corresponding to the α-particle energies of the ground-state and low-spin isomer decays of ^{155}Lu are indicated. (b) Energy spectrum of α particles following the implantation in the same DSSD pixel of an evaporation residue associated with a 759 keV γ ray emitted in the decay of the 19^- isomeric state in ^{156}Lu [34]. (c) Same as (b) but for the 1258 keV γ rays emitted in the decay of the isomeric state in ^{155}Hf identified in the present work. Background has been subtracted in (b) and (c) by selecting a region of the γ-ray spectrum above the respective selected transitions. The dotted lines indicate α-decay energies of ^{155,156}Lu and are drawn to guide the eye.

Figure 3 shows the energy spectra of γ rays observed in the Ge detectors at the focal plane of MARA within 8 μs of an evaporation-residue implantation into the DSSD that was followed within 4.5 s by an α decay of ^{155}Lu in the same pixel of the DSSD. The same γ rays can be seen when selecting on (a) α decays of the $\pi h_{11/2}$ state and (b) the $\pi s_{1/2}$ state of ^{155}Lu, although the spectrum of Fig. 3(b) is dominated by other γ-ray peaks that are attributed to decays of the known isomeric state in ^{156}Lu [34]. This isomer has a half-life of 179 ns and was strongly populated in the experiment. It feeds the $\pi h_{11/2}$ state in ^{156}Lu that decays by emitting 5565 keV α particles that satisfy the energy criterion set for the 5584 keV α decays of ^{155}Lu (see Fig. 2).

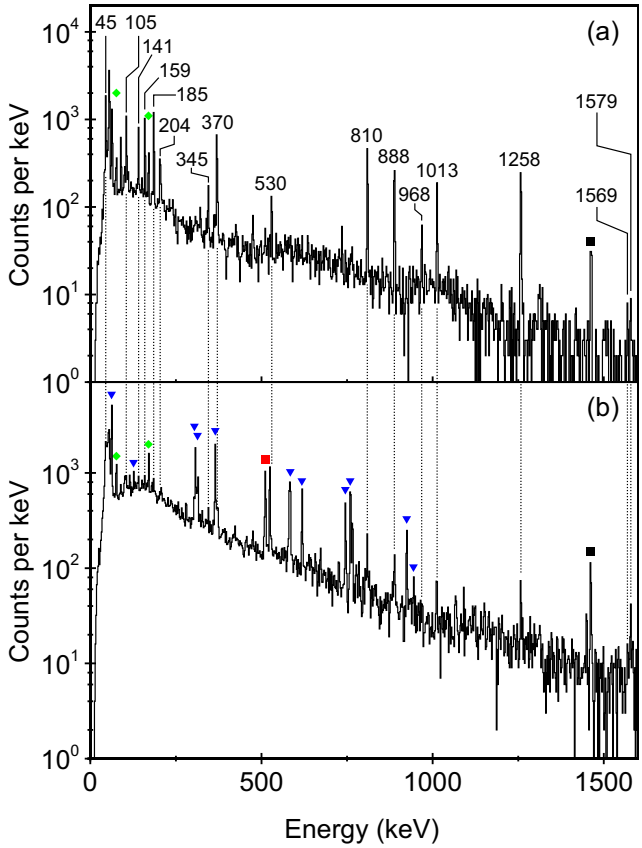

FIG. 3. Energy spectra of γ rays observed in the focal-plane Ge detectors within 8 μs of an evaporation-residue implantation into the DSSD that was followed within 4.5 s in the same DSSD pixel by (a) a 5655 keV α decay of the ground state of ^{155}Lu and (b) a 5584 keV α decay of the low-spin isomer of ^{155}Lu. A background spectrum of γ rays observed up to 8 μs *before* the implantation of these evaporation residues has been subtracted. Transitions assigned to ^{155}Hf are labeled with their energies in keV in (a) and the dotted lines are drawn to guide the eye to highlight the γ-ray peaks assigned to ^{155}Hf that appear in both spectra. The peaks at 76 and 170 keV indicated by the green diamonds are attributed to background from decays of the known 456 ns isomer in ^{158}Lu [42] that was strongly populated in this experiment. Peaks attributed to γ rays emitted in decays of the known 19^- isomer in ^{156}Lu [34] are indicated by the blue triangles. The peaks at 511 and 1460 keV indicated by the red and black squares, respectively, are from background. Other weak peaks that are unlabeled could not be definitively assigned.

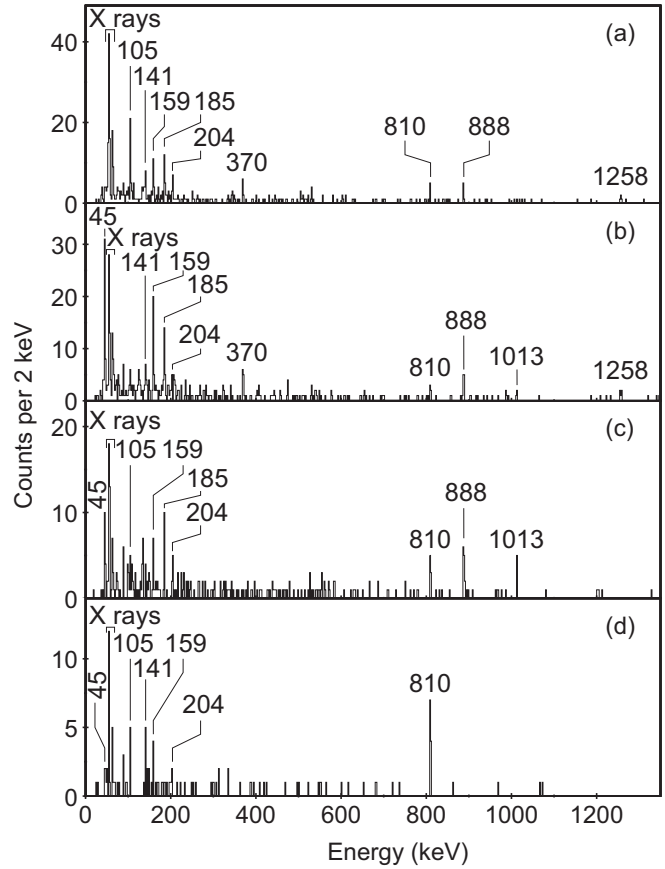

FIG. 4. Coincidence energy spectra of γ rays observed in the Ge detectors at the focal plane of MARA. All γ rays were recorded within 8 μs of an evaporation-residue implantation into the DSSD that was followed in the same DSSD pixel by a 5655 keV α decay within 4.5 s. The panels show coincidence spectra for γ rays of energy (a) 45 keV, (b) 105 keV, (c) 370 keV, and (d) 1258 keV. Hf K x-ray peaks are indicated and γ-ray peaks are labeled with their energy in keV.

Comparison of the distribution of evaporation residues correlated with the new γ-ray lines across the MARA focal plane with known α and isomer decays established that the isomer was from an $A = 155$ isobar. The atomic number was determined to be $Z = 72$ from analysis of the number of signals registered in JYTube in association with these evaporation residues. This assignment is supported by the energies of the K x-ray peaks in Fig. 3(a). On this basis, the γ rays are assigned as transitions depopulating an isomeric state in ^{155}Hf.

Further evidence in support of this assignment can be seen in Figs. 2(b) and 2(c), which show projections from a delayed coincidence matrix of γ rays emitted within 6.5 μs of an evaporation residue implanted into the DSSD and the subsequent α decays in the same DSSD pixel within 4.5 s. Figure 2(b) shows the clear α-decay peak of ^{156}Lu obtained when selecting 759 keV γ rays emitted in the decay of its 19^- isomeric state, while Fig. 2(c) is the corresponding spectrum obtained for the 1258 keV γ rays assigned to the decay of the isomeric state in ^{155}Hf. The α decays of both the ground state and low-spin isomeric state in ^{155}Lu are evident in the latter spectrum, as would be expected following the β decay of ^{155}Hf [27].

The data were used to construct a γ-γ coincidence matrix from events selected using correlations with the 5655 keV α decay of the ground state of ^{155}Lu. Examples of coincidence spectra are shown in Fig. 4. Panel (a) shows the energy spectrum of γ rays observed in coincidence with those in the peak at 45 keV, in which many of the γ-ray peaks visible in Fig. 3(a) can be seen. It is worth noting that this peak at 45 keV

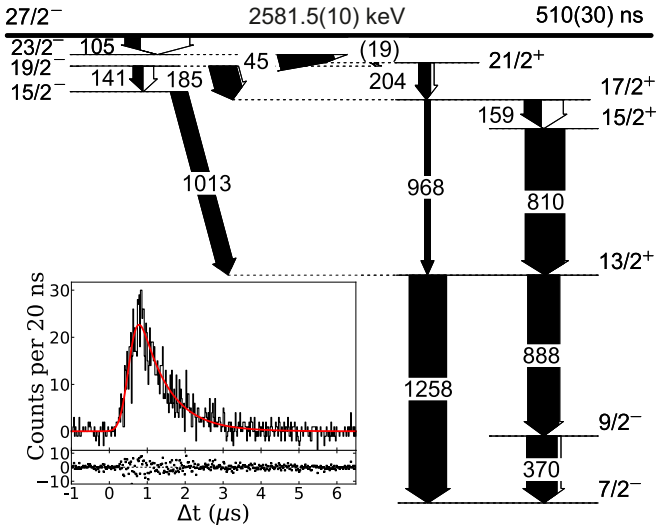

FIG. 5. The proposed decay scheme of the $27/2^-$ isomeric state in ^{155}Hf. All spin-parity assignments are tentative. The arrow widths are proportional to the transition intensities, with the black portion indicating the γ-ray intensity. The unobserved 18.8 keV transition is included tentatively in the level scheme to account for the observation of 141 and 185 keV γ rays in coincidence with the 45 keV transition. The upper panel of the inset in the bottom left corner shows the decay curve for the 105 keV transition measured with the BEGe detectors, with the red line showing the fit to the data assuming an exponential decay convoluted with a Gaussian function to model the detector timing response. The lower panel shows the fit residuals.

TABLE I. Gamma-ray energies, multipolarity assignments and intensities relative to that of the 45.3 keV transition for transitions below the $27/2^-$ isomer in ^{155}Hf. The intensities in column 4 have been corrected for internal conversion using BRICC [43] assuming pure multipolarities presented in column 3 and the γ-ray detection efficiencies simulated using the observed distribution of ^{155}Hf decays in the DSSD.

Energy (keV)	Intensity (%)	Multipolarity	Intensity (%) (ICC corrected)
45.3(5)	100(14)	$E1$	100(14)
105.4(5)	28(8)	$E2$	70(21)
140.9(5)	18(3)	$E2$	23(4)
159.5(5)	31(5)	$M1$	41(7)
185.5(5)	49(9)	$E1$	34(6)
204.3(5)	22(4)	$E2$	18(3)
344.6(5)	10(2)		
369.6(5)	56(9)	$M1$	39(6)
529.8(6)	14(4)		
809.5(5)	71(13)	$M1$	46(8)
888.3(5)	57(10)	$M2$	37(7)
968.5(6)	11(2)	$E2$	7(1)
1013.1(6)	31(6)	$E1$	20(4)
1257.7(6)	68(13)	$E3$	44(8)
1569.1(7)	6(1)		
1578.9(7)	7(2)		

is from a γ ray and does not arise from the escape of a Ge K x ray following photoelectric absorption of a Hf K x ray: no corresponding escape peak was observed in the energy spectra of the isomers of ^{156}Lu [34] or ^{158}Ta [35,36] that were also measured in this experiment.

Figure 4(b) shows γ rays in coincidence with the 105 keV transition, which also shows coincidences with many of the peaks in Fig. 3(a). Figures 4(c) and 4(d) show γ rays in coincidence with the 370 and 1258 keV transitions, respectively. These spectra demonstrate that the 370 and 888 keV transitions are in parallel with the 1258 keV transition. The excitation level scheme shown in Fig. 5 was constructed on the basis of γ-ray coincidence spectra and the intensities presented in Table I. The level of statistics was such that some of the transitions that might be expected from the level scheme did not appear in all of the coincidence spectra. For example, the 1013 keV transition is absent from Fig. 4(d), but from the number of counts in the 1258 keV peak and the Ge detector efficiency at 1013 keV, one would expect on average to observe only ≈4 counts.

From the analysis of the time differences between the implantation of the ^{155}Hf ions and the detection of 105 keV γ rays, the half-life of the isomeric state was measured as 510(30) ns (see inset to Fig. 5). The decay curve for the clover detector had lower statistics than that for the BEGe detectors, but yielded the same half-life within uncertainties. The effect of choosing different fitting functions for the Ge detector response is included in the uncertainty on the half-life.

Figure 6 shows the energy spectrum of prompt γ rays measured using the Ge detectors at the target position

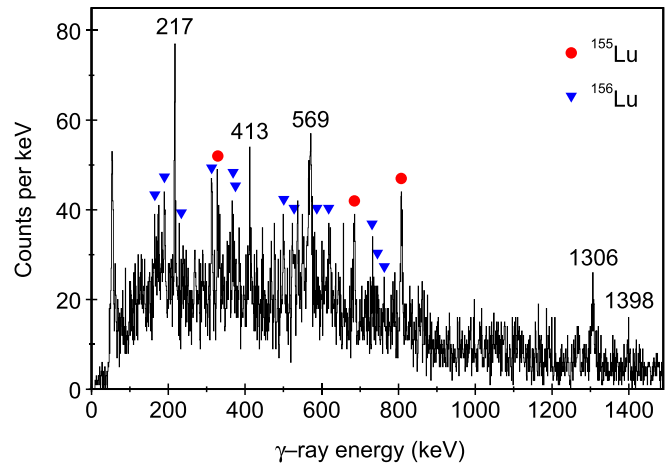

FIG. 6. Energy spectrum of prompt γ rays measured at the target position that were correlated with an evaporation residue implanted into the DSSD that was followed in the same DSSD pixel by a 5655 keV α decay within 4.5 s. A further requirement was that a γ ray from the decay of the seniority isomer in ^{155}Hf was detected in the Ge detectors at the focal plane of MARA within 8 μs of the ion implantation. Peaks assigned as γ-ray transitions populating the isomeric state in ^{155}Hf are labeled with their energies in keV. Contaminant peaks from the strongly produced nuclides ^{155}Lu [28] and ^{156}Lu [42] are indicated by the red circles and blue triangles, respectively.

TABLE II. Energies and efficiency-corrected intensities of γ-ray transitions populating the $27/2^-$ seniority isomer in ^{155}Hf. Intensities are normalized to that of the 569 keV transition.

Energy (keV)	Intensity (%)
217.1(6)	32(3)
412.9(8)	28(6)
569.2(8)	100(10)
1305.8(9)	68(8)
1397.5(9)	14(4)

associated with the delayed γ rays shown in Fig. 3(a). A few γ rays were identified that were not background from ^{155,156}Lu and are assumed to be transitions that populate the $27/2^-$ isomer in ^{155}Hf. The energies and relative intensities of these γ rays are presented in Table II. The level of statistics was insufficient to allow γ-ray coincidences to be analyzed, so a further experiment with a full array of Ge detectors will be required to confirm the assignments of these γ rays to ^{155}Hf and construct a level scheme above the isomer.

IV. DISCUSSION

The strongest transitions populating the $7/2^-$ ground states in the $N = 83$ isotones ^{149}Dy, ^{151}Er, and ^{153}Yb are stretched $E3$ decays from the yrast $13/2^+$ states [4,10,19–23]. The 1258 keV γ ray observed in this work is interpreted as the corresponding transition in ^{155}Hf. In the lighter isotones these $13/2^+$ states have half-lives of $\approx$10 ns, but it was not possible to measure a lifetime for this state in ^{155}Hf from the time stamps.

The excitation energy of the $13/2^+$ state in ^{155}Hf fits in well with the trend of increasing values with increasing Z [see Fig. 7(a)]. In ^{151}Er and ^{153}Yb, the yrast $9/2^-$ state drops below the $13/2^+$ state and opens up an alternative decay path to the ground state, which is also observed in ^{155}Hf. The excitation energy of this $9/2^-$ state also fits in well with the falling trend with increasing Z that extends to ^{157}W [46].

The strongest feeding of the $13/2^+$ state is from the 810 keV γ-ray transition, which is the second in the cascade of presumed $M1$ transitions from the $17/2^+$ state. Unlike in ^{149}Dy and ^{151}Er, this cascade is significantly more intense than the parallel stretched $E2$ transition. The excitation energy of the yrast $17/2^+$ state in ^{155}Hf is very similar to those in its isotones [see Fig. 7(a)], suggesting that it is likely to have a similar $\nu f_{7/2} \otimes 5^-$ structure. The $13/2^+$ state is also fed by a 1013 keV γ-ray transition that is assumed to be the counterpart of the $E1$ transition from the yrast $15/2^-$ state in ^{153}Yb. The placement of the 1013 keV transition in the level scheme was supported by the observation of coincident γ rays having energies of 141, 370, and 888 keV.

The transitions and energy levels discussed so far account for the strongest γ rays observed above 350 keV in Fig. 3(a). The lower-energy γ rays in this spectrum were considered as candidates for the expected $E2$ transition depopulating the $27/2^-$ isomer. The strongest of these γ rays has an energy of 45 keV, but if it were an $E2$ transition its intensity after allowing for internal conversion would be too high to match the intensities of γ rays feeding the ground state [43].

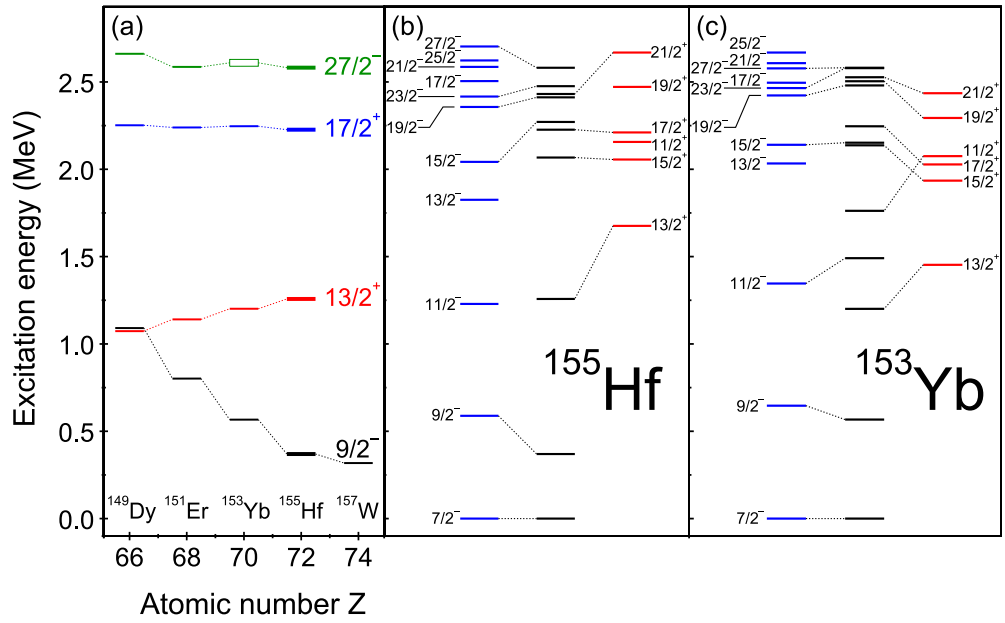

FIG. 7. (a) Systematics of excitation energies of yrast $9/2^-$, $13/2^+$, $17/2^+$, and $27/2^-$ levels above the $7/2^-$ ground states in odd-A $N = 83$ isotones for $Z = 66$–72. The data for $Z = 72$ shown by the thicker lines are derived from this study, while other data are taken from [10,20,44–46]. The rectangle represents the estimated range of likely values for the excitation energy of the $27/2^-$ state in ^{153}Yb. Comparison of yrast energy levels deduced from experiments with those from shell-model calculations for (b) ^{155}Hf and (c) ^{153}Yb. The experimental energy levels are in the center, with the negative-parity states to the left in blue and the positive-parity states to the right in red. The dotted lines connect the calculated energy levels with the associated observed levels. The experimental energy levels of ^{153}Yb are from [10,19], while those of ^{155}Hf are from the present work. See text for details of the shell-model calculations.

However, its intensity would be consistent within uncertainties if it were an $E1$ transition (see Table I). Given the coincidences with many other γ rays present in Fig. 4(a), the 45 keV γ-ray transition is interpreted as the counterpart of the $23/2^-$–$21/2^+$ transition in ^{153}Yb that has a similar energy [10,19].

A similar conclusion regarding intensity balances was reached for the 185 keV γ-ray transition, which is proposed as the $19/2^-$–$17/2^+$ transition. The next strongest unplaced γ ray has an energy of 105 keV. Its intensity after correcting for internal conversion assuming it is an $E2$ transition provides a good match for the total observed γ-ray intensity feeding the ground state. Other transitions do not have sufficient intensity, so the 105 keV γ-ray transition is proposed as the transition depopulating the $27/2^-$ isomer. With all these transitions placed in the level scheme there is a complete path to the ground state from the isomer, the excitation energy of which is deduced as 2581.5(10) keV.

Shell-model calculations were performed for ^{155}Hf and ^{153}Yb using the same approach as in Ref. [28], in which an inert ^{146}Gd core was assumed. The model space encompassed the proton $s_{1/2}$, $d_{3/2}$, and $h_{11/2}$ orbitals, and the neutron $h_{9/2}$, $f_{7/2}$, $f_{5/2}$, $p_{3/2}$, $p_{1/2}$, and $i_{13/2}$ orbitals. The realistic charge-dependent Bonn nucleon-nucleon potential [47] was renormalized using the perturbative G-matrix approach to take into account the core polarisation effect [48]. The monopole part of the effective interaction was further optimized by fitting to the excitation energies of 190 low-lying yrast states in $N =$ 82–86 nuclides in this region with a Monte Carlo optimization procedure [49]. Parts of the multipole interaction matrix elements were adjusted following the prescription of Ref. [50]. The single-particle energies were taken from experimental data: $\pi s_{1/2} = 0.0$ MeV, $\pi d_{3/2} = 0.253$ MeV, $\pi h_{11/2} =$ 0.0506 MeV, $\nu f_{7/2} = 0.0$ MeV, $\nu i_{13/2} = 0.997$ MeV, $\nu h_{9/2} =$ 1.397 MeV [51]. The unknown single-particle energies of the other neutron orbitals were determined by the fitting process. Calculations with this optimised interaction reproduced experimental energy levels of nuclei in this region with an average deviation of 190 keV [28].

The calculations for ^{155}Hf and ^{153}Yb are compared with the experimental data in Figs. 7(b) and 7(c), where it can also be seen that the excitation level schemes for these two isotones are expected to be similar. One transition that is absent in the level scheme for ^{155}Hf is the $E2$ transition between the $23/2^-$ and $19/2^-$ states, the counterpart of which in ^{153}Yb has an energy of 97 keV. This can be understood as being due to the long partial lifetime associated with its lower transition energy of 64 keV in ^{155}Hf. Observing a γ ray of this energy would also be hampered by interference from Hf K x rays. It was also not possible to assign the $9/2^-$ and $11/2^-$ states that would be expected at $\approx$1.5 MeV and are attributed to the $\nu f_{7/2} \otimes 2^+$ configuration [23]. The weak γ-ray lines at 1569 and 1579 keV are candidates for these, but there were insufficient statistics to establish their placement in the ^{155}Hf level scheme through coincidence measurements. It should also be noted that transitions with similar energies are known in the decays of microsecond isomers in ^{149,150}Er [6,15]. Overall the energy levels in ^{153}Yb (ten excited levels) and ^{155}Hf (nine excited levels) are reproduced by the calculations with average deviations of 180 and 200 keV, respectively.

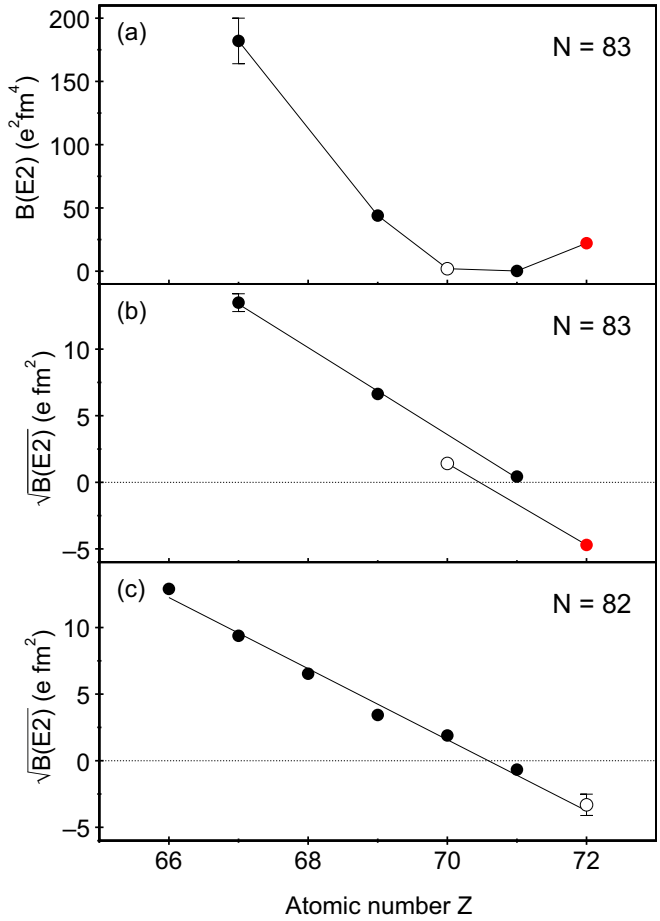

FIG. 8. (a) $B(E2)$ values for the isomeric transitions in $N = 83$ isotones plotted as a function of atomic number. The solid line joining the data points is drawn to guide the eye. $E2$ transition amplitudes $\sqrt{B(E2)}$ for (b) $N = 83$ and (c) $N = 82$ isotones. The solid lines show the average trends of the data (b) for the odd-Z isotones and for the even-Z isotones separately, and (c) for all isotones from ^{148}Dy to ^{153}Lu, inclusive. The values for the even-Z $N = 82$ isotones have been scaled up by a factor of 1.944 to account for the different geometric factors. The red data points denote the values for ^{155}Hf from the present work, while the hollow data points indicate estimated values for ^{153}Yb and ^{154}Hf, for which the transition energies are unknown. Other data are taken from refs. [3,4,6,7,9–11,15,24,25]. Error bars are plotted where they are larger than the symbol size.

The partial lifetime and energy of the 105 keV γ-ray transition depopulating the $27/2^-$ isomer in ^{155}Hf correspond to a reduced transition probability of $B(E2) = 0.45(3)$ W.u. or 22(2) e^2fm^4. This value is an order of magnitude larger than the value deduced for the corresponding transition in ^{153}Yb, establishing unambiguously that the minimum in $B(E2)$ values arising because of seniority cancellation has been passed [10,19]. This can be seen in Fig. 8(a), where the parabolic variation of $B(E2)$ values with Z expected from shell-model considerations can be seen borne out in the systematics for $N = 83$ isotones.

The shell-model calculations performed in the present work predict a $B(E2)$ value for ^{155}Hf of 119 e^2fm^4, which is substantially larger than the measured value. The corresponding calculated value of 37.5 e^2fm^4 for ^{153}Yb is also larger than the estimated value for that nuclide [10,19]. These differences may possibly point to the role of core excitations across the $Z = 64$ subshell gap that slightly shift the location of half occupancy of the $\pi h_{11/2}$ orbital, as discussed in Ref. [52].

Previous studies have shown that the isomeric $E2$ transition amplitudes $\sqrt{B(E2)}$ for isotonic chains around $N = 82$ vary approximately linearly with Z [9,10,24,25]. Assuming that the $B(E2)$ values are dominated by contributions from $\pi h_{11/2}$ configurations, one would expect that $\sqrt{B(E2)} \propto (2j + 1 - n)/(2j + 1 - \nu)$, where n is the occupation of the orbital being filled, j is its total angular momentum quantum number, and ν is the seniority. Figure 8(b) compares the present measurements for ^{155}Hf with the linear trend for the odd-Z $N = 83$ isotones, assuming there is a sign change for $\sqrt{B(E2)}$ around $Z = 71$, and for the odd-odd cases it is assumed that the unpaired neutron acts as a spectator. The corresponding trend for the $N = 82$ isotones is shown in Fig. 8(c), where the plotted values for the even-Z isotones have been adjusted for the expected geometric factors so that they are on the same scale. For both the $N = 82$ and $N = 83$ isotone chains, including the new datum for ^{155}Hf, the zero crossing point where the $\pi h_{11/2}$ orbital is half-filled is close to $Z = 71$. However, there is a slight shift between the trends for the $N = 82$ and odd-odd N= 83 isotones, an observation that has been ascribed to a $(\pi h^n_{11/2})_{27/2}\nu f_{7/2}$ component of the 15^+ states of the odd-odd nuclei, in addition to the $(\pi h^n_{11/2})_{23/2}\nu f_{7/2}$ component [25]. This mechanism might also explain the shift between the trends for the odd-Z and even-Z $N = 83$ isotones.

It is interesting to compare the behavior observed around $N = 82$ with that of states around $Z = 50$ formed by coupling $h_{11/2}$ neutrons. Similar seniority isomers involving $\nu h_{11/2}$ configurations have been observed in the chain of tin isotopes and the measured $E2$ transition amplitudes were found to vary linearly over a wide range of neutron numbers [53,54], with the $\nu h_{11/2}$ orbital becoming half-filled close to $N = 73$ [55]. For the Sb isotopes, which are analogous to the $N = 83$ isotones of interest in this work, the unpaired proton is thought to affect both the neutron seniority and the neutron angular-momentum mixing in the odd-A cases [56]. However, it should be noted that the unpaired particle is in a different orbital in the two regions and further measurements are probably required before a definitive conclusion on the importance of these effects near $N = 82$ can be reached.

V. SUMMARY AND CONCLUSIONS

The cascades of γ rays emitted in the decay of an isomeric state in ^{155}Hf have been identified and an excitation level scheme has been constructed. The isomer is assigned as a $27/2^-$ state similar to those in its lighter $N = 83$ isotones. The measured half-life of 510(30) ns and depopulating transition energy of 105.4 keV correspond to a $B(E2)$ value of 0.45(3) W.u. or 22(2) e^2fm^4. This $B(E2)$ value fits in well with the parabolic trend for $N = 83$ isotones, confirming that the $\pi h_{11/2}$ orbital is more than half filled above $Z = 71$. To determine whether the parabolic trend of $B(E2)$ values continues to heavier elements will require extending these isomer-decay measurements to even more exotic isotones. For the adjacent isotone ^{156}Ta [41,57] this should be feasible, provided the isomeric ratio and half-life are favorable. However, studying the heaviest currently known isotone ^{157}W [46] will be challenging because of the much lower expected production cross section.

ACKNOWLEDGMENTS

Financial support for this work was provided by the United Kingdom Science and Technology Facilities Council (STFC) through Grants No. ST/P004598/1, No. ST/V001027/1, and No. ST/V001035/1; the EU Seventh Framework Programme "Integrating Activities - Transnational Access," Project No. 262010 (ENSAR); by the Slovak Research and Development Agency (Contracts No. APVV-22-0282 and No. APVV-20-0532) and Slovak Grant Agency VEGA (Contracts No. 1/0651/21 and No. 2/0067/21); by the Research and Development Operational Programme funded by the European Regional Development Fund, Project No. ITMS code 26210120023 (20%); by the U.S. DOE under Contract No. DE-AC02-05CH11231 (LBNL); and by the Academy of Finland under the Finnish Centre of Excellence Programme 2012–2017 (Nuclear and Accelerator Based Physics Programme at JYFL). T.G. acknowledges the support of the Academy of Finland, Contract No. 131665. J.P. and S.S. acknowledge the Academy of Finland (Finland) Grant No. 307685. M.V. acknowledges funding from the ESET Foundation (Slovakia). The authors would like to express their gratitude to the technical staff of the Accelerator Laboratory at the University of Jyväskylä for their support. The authors would also like to thank the GSI Target Laboratory for providing the carbon reset foils.

[1] G. D. Dracoulis, P. M. Walker, and F. G. Kondev, Rep. Prog. Phys. **79**, 076301 (2016).
[2] B. Maheshwari and K. Nomura, Symmetry **14**, 2680 (2022).
[3] P. J. Daly, P. Kleinheinz, R. Broda, A. M. Stefanini, S. Lunardi, H. Backe, L. Richter, R. Willwater, and F. Weik, Z. Phys. A **288**, 103 (1978).
[4] P. J. Daly, P. Kleinheinz, R. Broda, S. Lunardi, H. Backe, and J. Blomqvist, Z. Phys. A **298**, 173 (1980).
[5] B. Haas *et al.*, Nucl. Phys. A **362**, 254 (1981).
[6] H. Helppi, Y. H. Chung, P. J. Daly, S. R. Faber, A. Pakkanen, I. Ahmad, P. Chowdhury, Z. W. Grabowski, T. L. Khoo, R. D. Lawson, and J. Blomqvist, Phys. Lett. B **115**, 11 (1982).
[7] D. Nisius, R. V. F. Janssens, I. G. Bearden, R. H. Mayer, I. Ahmad, P. Bhattacharyya *et al.*, Phys. Rev. C **52**, 1355 (1995).
[8] E. Nolte, G. Korschinek, and Ch. Setzensack, Z. Phys. A **309**, 33 (1982).

[9] J. H. McNeill, J. Blomqvist, A. A. Chishti, P. J. Daly, W. Gelletly, M. A. C. Hotchkis, M. Piiparinen, B. J. Varley, and P. J. Woods, Phys. Rev. Lett. **63**, 860 (1989).

[10] J. H. McNeill, A. A. Chishti, P. J. Daly, W. Gelletly, M. A. C. Hotchkis, M. Piiparinen, B. J. Varley, P. J. Woods, and J. Blomqvist, Z. Phys. A **344**, 369 (1993).

[11] J. Wilson, S. R. Faber, P. J. Daly, I. Ahmad, J. Borggreen, P. Chowdhury, T. L. Khoo, R. D. Lawson, R. K. Smither, and J. Blomqvist, Z. Phys. A **296**, 185 (1980).

[12] J. Kownacki, C. Droste, T. Morek, E. Ruchowska, M. Kisielinski, M. Kowalczyk *et al.*, Phys. Rev. C **81**, 044305 (2010).

[13] R. D. Lawson, Z. Phys. A **303**, 51 (1981).

[14] R. Broda, P. J. Daly, Z. W. Grabowski, H. Helppi, M. Kortelahti, J. McNeill, R. V. F. Janssens, R. D. Lawson, D. C. Radford, and J. Blomqvist, Z. Phys. A **321**, 287 (1985).

[15] R. Broda, P. J. Daly, J. McNeill, R. V. F. Janssens, and D. C. Radford, Z. Phys. A **327**, 403 (1987).

[16] D. Nisius, B. Fornal, I. G. Bearden, R. Broda, R. H. Mayer, Z. W. Grabowski *et al.*, Phys. Rev. C **47**, 1929 (1993).

[17] R. Broda, Y. H. Chung, P. J. Daly, Z. W. Grabowski, J. McNeill, R. V. F. Janssens, and D. C. Radford, Z. Phys. A **316**, 125 (1984).

[18] R. Broda, P. J. Daly, J. H. McNeill, Z. W. Grabowski, R. V. F. Janssens, R. D. Lawson, and D. C. Radford, Z. Phys. A **334**, 11 (1989).

[19] J. H. McNeill, A. A. Chisti, P. J. Daly, M. A. C. Hotchkis, M. Piiparinen, and B. J. Varley, Z. Phys. A **332**, 105 (1989).

[20] A. M. Stefanini, P. Kleinheinz, and M. R. Maier, Phys. Lett. B **62**, 405 (1976).

[21] J. Jastrzębski, R. Kossakowski, J. Łukasiak, M. Moszyński, Z. Preibisz, S. André, J. Genevey, A. Gizon, and J. Gizon, Phys. Lett. B **97**, 50 (1980).

[22] R. Barden, A. Płochocki, D. Schardt, B. Rubio, M. Ogawa, P. Kleinheinz, R. Kirchner, O. Klepper, and J. Blomqvist, Z. Phys. A **329**, 11 (1988).

[23] R. Collatz, P. Kleinheinz, C. T. Zhang, H. Keller, R. Kirchner, O. Klepper, and E. Roeckl, Z. Phys. A **359**, 115 (1997).

[24] J. H. McNeill, R. Broda, Y. H. Chung, P. J. Daly, Z. W. Grabowski, H. Helppi, M. Kortelahti, R. V. F. Janssens, T. L. Khoo, R. D. Lawson, D. C. Radford, and J. Blomqvist, Z. Phys. A **325**, 27 (1986).

[25] J. H. McNeill, J. Blomqvist, A. A. Chishti, P. J. Daly, W. Gelletly, M. A. C. Hotchkis, M. Piiparinen, B. J. Varley, and P. J. Woods, Z. Phys. A **335**, 241 (1990).

[26] S. Hofmann, G. Münzenberg, F. Heßberger, W. Reisdorf, P. Armbruster, and B. Thuma, Z. Phys. A **299**, 281 (1981).

[27] P. J. Sapple, R. D. Page, D. T. Joss, L. Bianco, T. Grahn, J. Pakarinen *et al.*, Phys. Rev. C **84**, 054303 (2011).

[28] R. J. Carroll, B. Hadinia, C. Qi, D. T. Joss, R. D. Page, J. Uusitalo *et al.*, Phys. Rev. C **94**, 064311 (2016).

[29] J. Sarén, The ion-optical design of the MARA recoil separator and absolute transmission measurements of the RITU gas-filled recoil separator, Ph.D. thesis, University of Jyväskylä, 2011.

[30] J. Sarén, J. Uusitalo, M. Leino, P. T. Greenlees, U. Jakobsson, P. Jones, R. Julin, S. Juutinen, S. Ketelhut, M. Nyman, P. Peura, P. Rahkila, C. Scholey, and J. Sorri, Nucl. Instrum. Methods Phys. Res., Sect. B **266**, 4196 (2008).

[31] J. Uusitalo, J. Sarén, J. Partanen, and J. Hilton, Acta Phys. Pol. B **50**, 319 (2019).

[32] J. Sarén, J. Uusitalo, and H. Joukainen, Nucl. Instrum. Methods Phys. Res., Sect. B **541**, 33 (2023).

[33] S. Agostinelli *et al.*, Nucl. Instrum. Methods Phys. Res., Sect. A **506**, 250 (2003).

[34] M. C. Lewis, E. Parr, R. D. Page, C. McPeake, D. T. Joss, F. A. Ali *et al.*, Phys. Rev. C **98**, 024302 (2018).

[35] R. J. Carroll, R. D. Page, D. T. Joss, J. Uusitalo, I. G. Darby, K. Andgren *et al.*, Phys. Rev. Lett. **112**, 092501 (2014).

[36] R. J. Carroll, R. D. Page, D. T. Joss, D. O'Donnell, J. Uusitalo, I. G. Darby *et al.*, Phys. Rev. C **93**, 034307 (2016).

[37] J. Henderson *et al.*, J. Instrum. **8**, P04025 (2013).

[38] J. Pakarinen *et al.*, Eur. Phys. J. A **56**, 149 (2020).

[39] I. H. Lazarus *et al.*, IEEE Trans. Nucl. Sci. **48**, 567 (2001).

[40] P. Rahkila, Nucl. Instrum. Methods Phys. Res., Sect. A **595**, 637 (2008).

[41] R. D. Page, P. J. Woods, R. A. Cunningham, T. Davinson, N. J. Davis, A. N. James, K. Livingston, P. J. Sellin, and A. C. Shotter, Phys. Rev. C **53**, 660 (1996).

[42] C. G. McPeake, Excited states in the exotic nuclei ^{156}Lu and ^{158}Lu, Ph.D. thesis, University of Liverpool, 2017.

[43] T. Kibédi, T. W. Burrows, M. B. Trzhaskovskaya, P. M. Davidson, and C. W. Nestor, Jr., Nucl. Instrum. Methods Phys. Res., Sect. A **589**, 202 (2008); https://bricc.anu.edu.au/.

[44] Y. A. Akovali, K. S. Toth, A. L. Goodman, J. M. Nitschke, P. A. Wilmarth, D. M. Moltz, M. N. Rao, and D. C. Sousa, Phys. Rev. C **41**, 1126 (1990).

[45] T. Komppa, R. Komu, M. Kortelahti, J. Muhonen, A. Pakkanen, M. Piiparinen, I. Prochazka, and J. Blomqvist, Z. Phys. A **314**, 33 (1983).

[46] L. Bianco *et al.*, Phys. Lett. B **690**, 15 (2010).

[47] R. Machleidt, Phys. Rev. C **63**, 024001 (2001).

[48] M. Hjorth-Jensen, T. T. S. Kuo, and E. Osnes, Phys. Rep. **261**, 125 (1995).

[49] C. Qi and Z. X. Xu, Phys. Rev. C **86**, 044323 (2012).

[50] A. Algora, B. Rubio, D. Cano-Ott, J. L. Tain, A. Gadea, J. Agramunt *et al.*, Phys. Rev. C **68**, 034301 (2003).

[51] National Nuclear Data Center, information extracted from the NuDat 2 database, http://www.nndc.bnl.gov/nudat2/.

[52] T. Matsuzawa, H. Nakada, H. Ogawa, and G. Momoki, Phys. Rev. C **62**, 054304 (2000).

[53] R. H. Mayer *et al.*, Phys. Lett. B **336**, 308 (1994).

[54] Ł. W. Iskra, R. Broda, R. V. F. Janssens, C. J. Chiara, M. P. Carpenter, B. Fornal *et al.*, Phys. Rev. C **93**, 014303 (2016).

[55] R. Broda *et al.*, Phys. Rev. Lett. **68**, 1671 (1992).

[56] S. Biswas *et al.*, Phys. Rev. C **99**, 064302 (2019).

[57] I. G. Darby, R. D. Page, D. T. Joss, L. Bianco, T. Grahn, D. S. Judson *et al.*, Phys. Rev. C **83**, 064320 (2011).